

Original Research

# Modulation of Mitochondrial Dynamics in Primary Hippocampal Cultures of 5xFAD Mice by Mdivi-1, MFP, and Exogenous Zinc

Alina Chaplygina<sup>1,\*</sup>, Daria Zhdanova<sup>1</sup>

<sup>1</sup>Institute of Cell Biophysics, Russian Academy of Sciences—a Separate Division of Federal Research Center Pushchino Research Center for Biological Studies, Russian Academy of Sciences (ICB RAS), 142290 Pushchino, Russia

\*Correspondence: [shadowhao@yandex.ru](mailto:shadowhao@yandex.ru) (Alina Chaplygina)

Academic Editor: Hongquan Wang

Submitted: 8 July 2025 Revised: 27 August 2025 Accepted: 8 September 2025 Published: 26 September 2025

## Abstract

**Background:** Mitochondrial dynamics—the balance between fission, fusion, and mitophagy—are essential for maintaining cellular homeostasis and are increasingly implicated in the pathogenesis of Alzheimer’s disease (AD). **Methods:** Here, we investigated the effects of targeted modulation of mitochondrial fission and fusion on mitochondrial morphology and metabolic status in primary hippocampal cultures derived from 5xFAD transgenic mice. Mitochondrial dynamics were modulated using the fission inhibitor Mitochondrial Division Inhibitor 1 (Mdivi-1), the fusion promoter mitochondrial fusion promoter M1 (MFP M1), and exogenous zinc as a fission activator. We evaluated mitochondrial morphology, lipofuscin accumulation, beta-amyloid (A $\beta$ 42) levels, and reactive oxygen species (ROS). The general condition of the cultures was assessed morphologically using neuronal and astrocytic markers. **Results:** Modulating mitochondrial dynamics altered mitochondrial morphology, decreased A $\beta$ 42, lipofuscin, and ROS levels, and improved cellular organization. Treatments with MFP and Mdivi-1 promoted mitochondrial hyperfusion without complete network integration and were associated with reduced astrogliosis and increased neuronal density. In contrast, zinc induced dose-dependent mitochondrial fragmentation and astrocytic clasmatodendrosis, with lower concentrations enhancing A $\beta$  clearance and higher concentrations inducing toxicity. **Conclusions:** Mitochondrial fusion and fission significantly influence lipofuscin and amyloid accumulation in 5xFAD cultures, underscoring their potential as therapeutic targets in neurodegenerative diseases. We propose that mitochondrial morphology acts as a key regulator of both cellular homeostasis and disease pathology.

**Keywords:** mitochondria; mitochondrial fusion; mitochondrial fission; mitochondrial dynamic; Alzheimer’s disease; lipofuscin; primary cell culture

## 1. Introduction

Alzheimer’s disease (AD) has a complex etiology, with mitochondrial dysfunction extensively studied as a potential contributing factor [1]. Mitochondrial dysfunction, particularly related to bioenergetics and its impact on neuronal fate and degeneration, is recognized as one of the most critical factors in the pathogenesis of AD [2].

Mitochondria undergo fusion in response to increased energy demands or fission to isolate and eliminate damaged mitochondria via mitophagy [3]. This sequence of processes is referred to as mitochondrial dynamics, and maintaining a proper balance among fusion, fission, and mitophagy is essential for optimal cellular function [4,5]. Disruptions in mitochondrial dynamics and clearance can lead to chronic energy dysregulation, contributing to oxidative stress, accumulation of neurotoxic proteins such as beta-amyloid (A $\beta$ ), and impaired cellular homeostasis [6,7].

Mitochondria exhibit remarkable variability in shape and structural organization within cells [8]. Each distinct mitochondrial morphology plays a critical role in different cellular processes, reflecting cell-type-specific adaptations in mitochondrial function [9–11]. Mitochondrial fusion is traditionally associated with enhanced adenosine triphos-

phate (ATP) production due to increased cristae surface area, greater dimerization of ATP synthase, and more efficient oxidative phosphorylation [12,13]. However, in most studies, fused mitochondria refer to interconnected mitochondrial networks, rather than to hyperfused megamitochondria, which, although present in primary cultures, are much less common. Notably, giant mitochondria are more frequently described in other tissues [14,15]. Mitochondrial fission, in contrast, is associated with cellular stress and degeneration [16], and excessive fragmentation has been observed in patients with Alzheimer’s disease and in various model organisms [17–20].

A $\beta$  infiltrates mitochondria, leading to the release of reactive oxygen species (ROS) and respiratory chain dysfunction [21,22]. In the mitochondria of patients with AD, A $\beta$  accumulation is closely associated with the formation of lipofuscin (LF), a pigment linked to cellular aging that is highly resistant to degradation [23]. Lipofuscin is believed to form due to incomplete lysosomal detoxification, leaving behind insoluble inclusions—many containing immunoreactive A $\beta$  peptide [24,25]. Disruption of mitochondrial dynamics results in mitochondrial dysfunction and decreased ATP production [26–29], ultimately leading to an



energy deficit in neurons [30,31]. Elevated A $\beta$  levels further contribute to oxidative stress and impaired intracellular signaling, creating a vicious cycle of pathology [32]. Under conditions of chronic stress, astrocytes fail to adequately clear A $\beta$  and support neuronal survival, exacerbating neuroinflammation and disease progression [33–35]. Impaired mitochondrial dynamics are increasingly recognized as either a potential precursor to A $\beta$  accumulation [36,37], or a downstream consequence of A $\beta$  pathology [38]. These observations suggest that mitochondria may act as central regulators of early pathological events in AD. Targeting mitochondrial dynamics is now considered a promising strategy in both cellular and medical research [39–41]. Manipulating these processes holds potential for improving mitochondrial function and restoring cellular metabolism in response to stress or disease-related dysfunction [42–45].

This study investigates the regulation of mitochondrial fusion and fission in primary astrocyte-neuron co-cultures derived from the hippocampi of 5xFAD transgenic mice. These mice serve as a genetic model of AD, mimicking the accumulation of pathological A $\beta$  in neurons. Notably, mutation-specific changes in mitochondrial morphology, function, and dynamics occur in these mice before the onset of neurological symptoms [46]. Progressive changes in mitochondrial dynamics and function have been observed in the hippocampus of 5xFAD mice as early as 2 months of age [47]. These mice exhibit significant synaptosomal mitochondrial dysfunction, characterized by an imbalance in mitochondrial dynamics skewed towards fission. Excessive fission negatively impacts energy production by compromising cristae integrity and the assembly of oxidative phosphorylation complexes, while reduced fusion hinders mitochondrial repair and increases the number of dysfunctional organelles. This imbalance could ultimately lead to synaptic dysfunction and neuronal death [6,48].

This study explores the effects of a Mitochondrial Division Inhibitor 1 (Mdivi-1), a Mitochondrial Fusion Promoter M1 (MFP M1), and a low-concentration zinc chloride solution (Zn) as a fission activator. Mdivi-1 is a cell-permeable quinazolinone compound, recognized as a mitochondrial fission inhibitor targeting the evolutionarily conserved mitochondrial GTPase Dnm1/Drp1 (dynamin-related GTPase/dynamin-like protein 1), a key regulator of mitochondrial fission, and has demonstrated neuroprotective effects in AD models [49–52]. However, its effects are not entirely straightforward: in addition to inhibiting Drp1, Mdivi-1 may increase ROS production, trigger mitochondrial retrograde signaling, and inhibit mitochondrial complex I [53,54]. In contrast, MFP M1 is a cell-permeable phenylhydrazonone compound [55], that enhances MFN2 (mitofusin-2) expression, a key protein involved in outer mitochondrial membrane fusion. MFP M1 has been shown to reduce brain mitochondrial dysfunction [56], particularly in tauopathy models [57]. In our study, zinc chloride was used to modulate mitochon-

drial fission. Exogenous zinc colocalizes with mitochondria [58], and its accumulation triggers Drp1-dependent fission through the Zip1 transporter, which interacts with Drp1 [59–61]. Zinc-induced mitochondrial fission is toxic, often promoting ROS production and mitochondrial fragmentation [62,63]. Fragmentation amplifies oxidative stress by increasing electron leakage from the respiratory chain, whereas enhanced fusion stabilizes the mitochondrial network and reduces ROS levels.

We also evaluate how these mitochondrial modulators affect ROS levels as part of the broader cellular stress response. Identifying compounds that selectively promote mitochondrial fission remains a challenge. While fission can be physiologically beneficial, it is often observed in pathological contexts—making therapeutic induction of fission a complex process. Moreover, mitochondria may undergo fission in response to a wide range of stressors, further complicating the search for effective, specific fission activators [64–67]. For example, respiratory chain inhibitors and oxidative phosphorylation uncouplers can cause mitochondrial fragmentation [68,69].

Our previous study showed that manipulating mitochondrial dynamics can induce pathological features even in healthy cells [70]. Here, we evaluate the astrocyte-to-neuron ratio in our cultures before and after treatment with mitochondrial modulators. In addition, we examine levels of A $\beta$ 1–42, a central marker of Alzheimer’s pathology in 5xFAD models, and assess lipofuscin accumulation—a hallmark of mitochondrial dysfunction and impaired autophagy—as an indicator of metabolic stress [24,71,72]. We also measure ROS levels to assess oxidative damage. We hypothesize that controlled modulation of mitochondrial dynamics will alter A $\beta$  accumulation, oxidative stress, and metabolic imbalance in 5xFAD primary hippocampal cultures.

## 2. Materials and Methods

### 2.1 Animal Models

The animals used in this study were 5xFAD mice, a double transgenic model of Alzheimer’s disease. Neurons of 5xFAD mice, both *in vivo* and in culture, accumulate A $\beta$  from the beginning of life. Mice of the 5xFAD line were bred on an SJL/C57B6 (Swiss James Lambert/C57 Black 6) congenic background to minimize concerns related to allelic segregation and the variability of the original hybrid strain. The transgenic mouse line was obtained from Charles River Laboratory (Wilmington, MA, USA). All experiments were conducted on F1 progeny generated by crossing transgene-positive animals with SJL/C57BL6 mice at the ICB RAS facility (Pushchino, Moscow region, Russia). 5xFAD transgenic mice express five familiar AD mutations: the *APP* (Amyloid Precursor Protein) (695) transgene carries the Swedish (K670N, M671L), Florid (I716V), and London (V717I) mutations, while the *PSEN1* (Presenilin 1) transgene carries M146L and L286V

mutations. Both transgenes are expressed under the murine *Thy1* (Thymocyte Differentiation Antigen 1) promoter, ensuring overexpression specifically in neurons. The transgenes are inserted at a single locus (Chr3:6297836), without disrupting known genes. Non-transgenic littermates served as controls. Genotyping was performed by PCR using DNA from ear biopsy specimens, with the presence of a 377-bp-long Tg cassette detected by primers 5'-AGG ACT GAC CAC CAC TCG ACC AG-3' and 5'-CGG GGG TCT AGT TCT TCT GCA T-3', followed by electrophoretic visualization.

To minimize animal suffering, invasive procedures such as band surgery were avoided. Instead, natural delivery was used, followed by rapid guillotination of newborns *in vitro*, enabling hippocampal extraction for primary cultures. To reduce intra-litter variation, animals from different litters were used across the experiment. The experimental protocol was approved by the Bioethics Commission of ICB RAS (Approval ID: 1/032023, date: 2023-3-22).

## 2.2 Primary Hippocampal Culture

Mixed astro-neuronal cultures were established from 0–1-day-old mice to investigate cellular characteristics *in vitro*. The hippocampi were mechanically dissociated and treated with a Trypsin-EDTA solution (lot 25200056, Gibco, Waltham, MA, USA). The resulting cell suspension was transferred to wells coated with Poly-D-Lysine (A3890401, Gibco, USA) or to glass slides coated with the same substrate, to ensure adequate adhesion. After attachment, the cultures were maintained with Neurobasal Medium (21103049, Gibco, Waltham, MA, USA) supplemented with 2% B-27 (17504044, Gibco, Waltham, MA, USA) and 1% Penicillin-Streptomycin-Glutamine (10378016, Gibco, Waltham, MA, USA). Cells were incubated at 37 °C with 5% CO<sub>2</sub>, and cultures were harvested for experimentation after 14 days of maturation.

To increase heterogeneity, multiple hippocampi were pooled and mechanically divided into 4–5 fragments, minimizing variability linked to genetic and environmental factors within a single litter. The design aimed to reduce the number of animals used while ensuring sufficient biological replication. On average, each hippocampus yielded three biological replicates.

## 2.3 Visualization of Mitochondria

Mitochondria were visualized by transduction/transfection of cultures with the CellLight BacMam 2.0 Red system (C10600, Thermo Fisher Scientific, Waltham, MA, USA). This pre-constructed vector employs BacMam 2.0 technology to introduce a fluorescent protein fused to the E1-alpha-pyruvate dehydrogenase leader sequence. The reagent was applied according to the manufacturer's protocol and incubated with cells for 16 hours before use.

Mitochondrial morphology was assessed in live, unfixed cell cultures using a Leica DM IL LED microscope (Leica, Wetzlar, Germany) with a  $\times 100$  oil immersion objective. Fixation was avoided, and it caused significant artifacts in mitochondrial architecture (in **Supplementary Fig. 1**). All morphological data were obtained from live cells to preserve mitochondrial integrity and function. Because multicomponent primary cultures form multilayered network structures, quantification of mitochondrial morphology in neurons was challenging. In contrast, comparable analysis was feasible in astrocytes, providing insights into their mitochondrial characteristics. Mitochondrial area and length were estimated manually using ImageJ 1.54g software (National Institutes of Health, Bethesda, MD, USA). Images were calibrated with a known scale and mitochondrial length was measured using the straight tool. Areas were determined through polygonal selections of each individual mitochondrion. In cases of branching, all branches were included in the total length calculation. For circular or polygonal mitochondria, its maximum diagonal was used.

## 2.4 Effects on Mitochondrial Fusion and Fission Processes

Two compounds with different mechanisms were used to modulate mitochondrial dynamics. The first, Mdivi-1 (475856, Sigma-Aldrich, Saint Louis, MO, USA), is a cell-permeable quinazolinone compound that reversibly inhibits dynamin-like protein 1 (Drp1), a key fission GTPase. The second substance, MFP M1 (SML0629, Sigma-Aldrich, Saint Louis, MO, USA), is a cell-permeable hydrazone that promotes mitochondrial fusion without affecting endoplasmic reticulum (ER) and lysosomes morphology. Substances were applied according to the manufacturer's instructions. Cultures were analyzed at 1 day and 5 days post-treatment with Mdivi-1 (10  $\mu$ M) and MFP M1 (5  $\mu$ M). The 1-day point captured early responses (network reorganization, ATP production, oxidative stress), while the 5-day point revealed sustained effects and adaptations.

Since no direct fission activators are commercially available, zinc chloride (Z0152, Sigma Aldrich, Saint Louis, MO, USA) was used in PBS at high (1  $\mu$ M) and low (0.1  $\mu$ M) concentrations. High concentrations caused pronounced mitochondrial and cellular stress; therefore, experiments were limited to 1 day. Low concentrations were used to modulate morphology without acute toxicity, with both 1-day and 5-day assessments performed.

## 2.5 Protein Concentration (UV Spectroscopy)

Protein concentrations were normalized using Lowry's method combined with UV spectroscopy [73]. The absorbance peak of tryptophan-containing proteins at 286 nm was recorded with a spectrophotometer Perkin Elmer MPF-44B (Perkin Elmer, Waltham, MA, USA). Calibration curves were generated from known protein standards, plotting concentration against absorbance.

## 2.6 Lipofuscin Detection

Lipofuscin, an autofluorescent pigment, was quantified spectrofluorimetrically as a marker for cellular metabolic stress. Primary hippocampal cultures were washed three times with PBS, then transferred to 5% sodium dodecyl sulfate (SDS). Samples were agitated for 5 minutes on a cooled shaker, lysed, and frozen for later use. Protein concentrations were normalized to 50 µg per sample. Lipofuscin was detected by its emission peak at ~450 nm upon excitation at 360 nm, measured with a Perkin Elmer MPF-44B spectrofluorimeter (Perkin Elmer, Waltham, MA, USA), gain  $\times 2$ , monochromator slits 5/5, with multipass mirror micro cuvettes designed for measuring the fluorescence of weakly absorbing solutions.

## 2.7 ELISA for A $\beta$ -staining

A $\beta$ 1-42 levels in cell cultures were quantified using the High Sensitive ELISA Kit for Amyloid Beta Peptide 1-42 (HEA946Hu, USCN Life Inc., Wuhan, Hubei, China), following the manufacturer's instructions for all experimental procedures. Primary hippocampal cultures were washed three times with PBS and lysed in PBS containing 1% TRITON-X, protease inhibitors (Protease Inhibitor MixM, P180239, Serva, Heidelberg, Germany), and phosphatase inhibitors (Phosphatase Inhibitor Mix I, P170262, Serva, Heidelberg, Germany). Protein concentrations were normalized to 20 µg per sample. Optical density at 450 nm was measured using a Multiskan FC microplate reader (Thermo Fisher Scientific, Waltham, MA, USA), and the concentrations of A $\beta$ 1-42 were calculated from standard curves.

## 2.8 ROS Detection

Mitochondrial superoxide was measured with MitoSox-red (M36008, Invitrogen, Carlsbad, CA, USA), according to the manufacturer's protocol. After treatment with test compounds, culture medium was changed, and cultures were incubated with 2.5 µM MitoSox-red for 20 minutes, then washed and analyzed with a fluorimetric plate reader (Agilent Technologies, Inc., Santa Clara, CA, USA).

## 2.9 Immunocytochemistry

For of neurons and astrocytes markers, cell cultures were fixed for 10 minutes in 4% paraformaldehyde. Membrane permeability was increased with 0.2% Triton X-100, and nonspecific binding to antigens was blocked in PBST (PBS + 0.1% Tween 20) with 1% BSA, 10% normalized donkey serum (ab7475, Abcam, Cambridge, UK), and 5% normalized goat serum (31872, Invitrogen, Carlsbad, CA, USA) for 1 hour at room temperature. Cultures were incubated overnight at 4 °C with primary antibodies, followed by fluorescent secondary antibodies for 2 hours at room temperature. Cells were washed 3 times with PBS (pH 7.4) for 5 minutes between steps. The following primary and secondary antibodies were used to stain for

neurons—Anti-MAP2 (microtubule-associated protein 2) antibody (ab32454, Abcam, Cambridge, UK, 1:200) and corresponding Alexa 594 nm (ab150080, Abcam, Cambridge, UK, 1:400); astrocytes—Anti-GFAP (glial fibrillary acidic protein) antibody (ab4674, Abcam, Cambridge, UK, 1:800); Alexa 488 nm (ab150169, Abcam, Cambridge, UK, 1:1000).

Imaging was acquired with a JuLI Stage fluorescence microscope (NanoEntek, Seoul, South Korea). Background correction was applied with the microscope's software to ensure uniform illumination and contrast. Images were analyzed in ImageJ software. To quantify neuronal and astrocytic contributions, images were processed with ImageJ algorithms and converted into binary black-and-white format. The total image area was defined as 100%, and the fraction occupied by immunopositive structures was expressed as a percentage of this total.

## 2.10 Statistical Analysis

Image analysis was performed in ImageJ. Statistical analyses were conducted in SigmaPlot 12.5 (Grafiti LLC, Palo Alto, CA, USA) and OriginPro 10.1.0.178 (OriginLab Corporation, Northampton, MA, USA). Data in the text are presented as mean  $\pm$  SD. For datasets with a small number of observations, results are shown as bar plots (mean  $\pm$  SD); for datasets with more than 50 observations, violin plots were used. Mitochondrial morphology is additionally represented as histograms with distribution curves estimated using the Kernel Smoothing nonparametric method. Normality was tested with the Shapiro–Wilk test. One-way ANOVA or Kruskal–Wallis test was used for group comparison, followed by Bonferroni's or Dunn's post hoc tests.

# 3. Results and Discussion

## 3.1 Modulated Mitochondrial Fusion and Fission.

Analysis of mitochondrial morphology revealed that mitochondria in 5xFAD (tg) cultures were, on average, longer, had a larger area, and displayed greater heterogeneity compared to those in non-transgenic (ntg) cultures (Fig. 1). In ntg cultures, mitochondrial lengths were tightly distributed within  $6.5 \pm 3.3$  µm (max 19 µm, min 0.12 µm). In contrast, transgenic cultures exhibited a pronounced tail in the distribution, with mitochondrial lengths extending up to 20–30 µm (near  $8 \pm 6.3$  µm, max 30 µm, min 0.5 µm). Similarly, tg mitochondria displayed a broader range of areas ( $0.1$  to  $3$  µm<sup>2</sup>), whereas ntg mitochondria were more compact, generally not exceeding ~6 µm<sup>2</sup>. These findings suggest that mitochondria in ntg cultures are more homogeneous in both shape and size, reflecting a baseline state of mitochondrial homeostasis, while 5xFAD cultures demonstrate disrupted mitochondrial dynamics, characterized by the coexistence of abnormally large and small mitochondria.

We next examined whether modulation of fusion and fission could alter these pathological features. Treatment



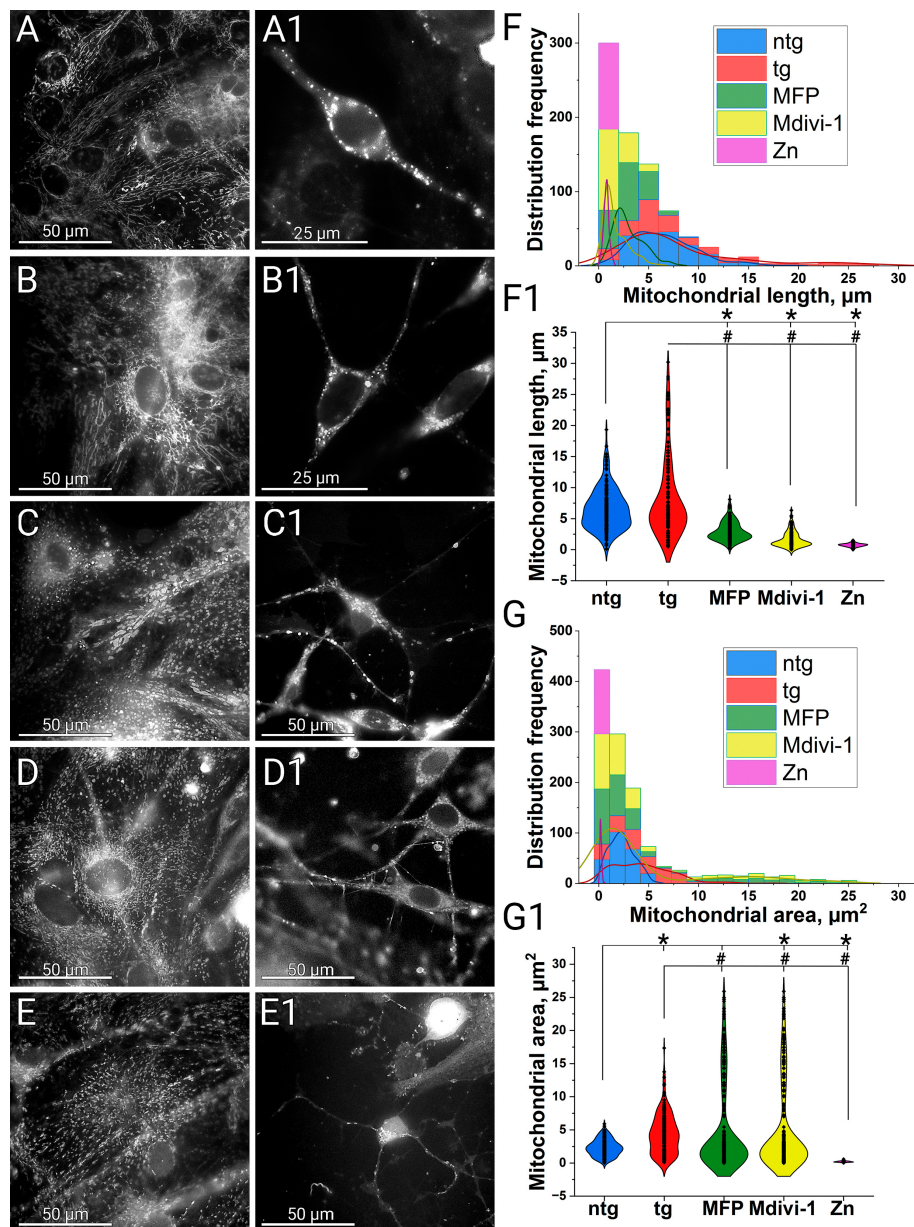


**Fig. 1. Modulation of mitochondrial fusion and fission.** Comparison of mitochondrial morphology in ntg and 5xFAD cultures and its alteration after treatment with Mdivi-1, MFP M1 and zinc. Mitochondria staining was performed by transfection/transduction with the CellLight BacMam 2.0 system. Mitochondrial morphology was examined on a Leica DM IL LED microscope using a  $\times 100$  oil-immersion objective. (A) Mitochondrial network in healthy nontransgenic astrocytes. Scale bar = 50  $\mu\text{m}$ . (A1) Mitochondria in healthy neuron. Scale bar = 25  $\mu\text{m}$ . (B) Mitochondrial network in 5xFAD astrocytes. Scale bar = 50  $\mu\text{m}$ . (B1) Mitochondria in 5xFAD neurons. Scale bar = 25  $\mu\text{m}$ . (C) Action of Mdivi-1 breaks down the mitochondrial network in 5xFAD astrocytes. Scale bar = 50  $\mu\text{m}$ . (C1) Action of Mdivi-1 reduces the number of tiny mitochondria in 5xFAD neurons. Scale bar = 50  $\mu\text{m}$ . (D) MFP M1 action converts the mitochondrial network in 5xFAD astrocytes to a pool of fused and hyperfused mitochondria, while the smallest mitochondria are retained. Scale bar = 50  $\mu\text{m}$ . (D1) MFP M1 action increases mitochondrial size in 5xFAD neurons. Scale bar = 50  $\mu\text{m}$ . (E) Action of exogenous zinc breaks the mitochondrial network in 5xFAD astrocytes into unstructured fragments. Scale bar = 50  $\mu\text{m}$ . (E1) Action of exogenous zinc in 5xFAD neurons leads to a decrease in mitochondrial size. Scale bar = 50  $\mu\text{m}$ . (F) Distribution histogram of mitochondrial lengths in astrocytes across experimental groups, overlaid with a Kernel density estimation curve. (F1) Violin plot of mitochondria length distribution in astrocytes. (G) Distribution histogram of mitochondrial areas in astrocytes across experimental groups, overlaid with a Kernel density estimation curve. (G1) Violin plot of mitochondria area distribution in astrocytes. \*  $p \leq 0.05$ , ANOVA, Dunn test, versus nontransgenic group (blue), #  $p \leq 0.05$ , ANOVA, Dunn test, versus transgenic 5xFAD group (red). MFP M1, Mitochondrial Fusion Promoter M1; ntg, cultures derived from nontransgenic animals; Mdivi-1, Mitochondrial Division Inhibitor 1.

with MFP M1 led to defragmentation of the mitochondrial network, with an average mitochondrial length of  $3 \pm 1.5 \mu\text{m}$  (max  $8 \mu\text{m}$ , min  $0.3 \mu\text{m}$ ). This was accompanied by an increase in the number of morphologically fused mitochondria that did not integrate into a continuous network, while a population of small mitochondria was retained (area range  $0.02\text{--}26 \mu\text{m}^2$ ). Although mitochondrial fusion is usually associated with the formation of a highly interconnected network, our observations indicate that fusion at the organelle level does not necessarily translate into increased network connectivity at the cellular level. After MFP M1 treatment, fused structures emerged, but without a corresponding increase in network organization. Instead, mitochondria were more diffusely distributed, forming isolated fused units alongside small individual mitochondria. Thus, mitochondrial fusion is a molecular event; mitochondrial networking is a higher-order spatial outcome. While often correlated, the two processes can become dissociated, and the presence of hyperfused mitochondria without network integration may suggest a cellular attempt to “repair” individual mitochondria rather than assemble them into a functional ensemble. Formation of megamitochondria is considered an adaptive response [74], and, as we will show in Section 3.3, this mechanism appears to support culture viability in 5xFAD.

We initially expected Mdivi-1 treatment to promote mitochondrial elongation and network formation. However, under our conditions, Mdivi-1 induced mitochondrial network defragmentation in astrocytes, with an average mitochondrial length of  $1.6 \pm 1.2 \mu\text{m}$  (max  $6.3 \mu\text{m}$ , min  $0.02 \mu\text{m}$ ) and an average area of  $1.4 \pm 1.0 \mu\text{m}^2$  (max  $7 \mu\text{m}^2$ , min  $0.03 \mu\text{m}^2$ ).

One possible explanation is that Mdivi-1 is not a strictly selective inhibitor of Drp1 GTPase but also suppresses respiratory chain complex I, an effect independent of Drp1 and not associated with mitochondrial elongation [75]. Consistently, the same authors showed that Mdivi-1 did not alter mitochondrial morphology in COS-7 cells after 24 h and did not prevent staurosporine-induced fragmentation, supporting the view that its effects are not Drp1-specific. Additionally, Mdivi-1 has been shown to reduce mitochondrial membrane potential and ATP synthesis while altering calcium homeostasis [54]. A decline in membrane potential activates the mitochondrial metalloendopeptidase *OMA1* (OMA1 protease) [76], which cleaves *OPA1* mitochondrial dynamin like GTPase (*OPA1*) and disrupt inner membrane fusion, potentially driving passive network dispersal despite Drp1 inhibition.

Another possibility involves Drp1-independent fission during mitophagy. Although Drp1 is central to mitochondrial fission, residual fragmentation persists even in its absence, suggesting alternative pathways for mitochondrial division [77,78]. A Drp1-independent fragmentation pathway has also been described, during mitophagy, in coordination with isolation membrane and autophagosome for-

mation [79]. Although mitophagy was not directly assessed here, the fragmentation observed with Mdivi-1 may reflect adaptive remodeling to facilitate turnover of dysfunctional organelles rather than stress-induced damage. Importantly, because Mdivi-1 does not block fusion, mitochondria can rejoin the network, preserving some plasticity. In parallel, chronic amyloid stress in 5xFAD may enhance actin- and endoplasmic reticulum (ER)-dependent mitochondrial constriction, a pathway independent of Drp1, that involves remodeling of ER-mitochondria contacts and actin polymerization, leading to constriction and fragmentation [80,81].

Finally, metabolic side effects of Mdivi-1 may indirectly suppress fusion through MFN1/2 degradation, *OPA1* proteolysis, altered oxidative phosphorylation (OXPHOS) protein expression, and increased superoxide production [82], collectively favoring fragmented mitochondrial forms. A transient response is also possible, with initial fission inhibition inducing hyperfusion, followed by a compensatory rebound fission as the drug is metabolized or inactivated. These mechanisms are not mutually exclusive and likely interact to produce the complex phenotype observed.

To further modulate fission, we applied exogenous zinc chloride. At high concentrations, zinc acted primarily as a toxicant, whereas lower concentrations produced morphologically evident fission without immediate neurite damage. Zinc exposure caused nearly complete mitochondrial network fragmentation into small elements that, under our experimental conditions, could not always be reliably dissolved. The average mitochondrial length was  $0.7 \pm 0.3 \mu\text{m}$  (max  $1.5 \mu\text{m}$ , min  $0.02 \mu\text{m}$ ), with an average area of  $0.2 \pm 0.08 \mu\text{m}^2$  (max  $0.5 \mu\text{m}^2$ , min  $0.04 \mu\text{m}^2$ ). Unlike MFP M1 and Mdivi-1, which produced heterogeneous populations of elongated and fragmented mitochondria, zinc induced a uniform pattern of small mitochondrial fragments. Mitochondria exposed to high-dose zinc underwent a striking morphological transition into evenly sized, punctate fragments, consistent with the activation of a non-physiological, potentially stress-induced fission mechanism. This uniform fragmentation sharply contrasts with the more heterogeneous remodeling observed under pharmacological modulation of fission or fusion, where mitochondrial morphology remains diverse and adaptive.

### 3.2 Determination of Lipofuscin, Beta-amyloid and ROS-level

Next, we assessed the levels of lipofuscin, ROS, and A $\beta$  in all the samples tested (Fig. 2).

As expected, untreated 5xFAD transgenic cultures exhibited significantly higher lipofuscin accumulation ( $570.9 \pm 16$  r.e.) compared to nontransgenic controls ( $345 \pm 14.3$  r.e.). Fluorescence intensity in the MFP M1—1 day group ( $289.6 \pm 7$  r.e.) was already lower than in both untreated transgenic cultures and nontransgenic controls, while by day 5 (MFP5:  $153.5 \pm 5$  r.e.), lipofuscin accumulation had

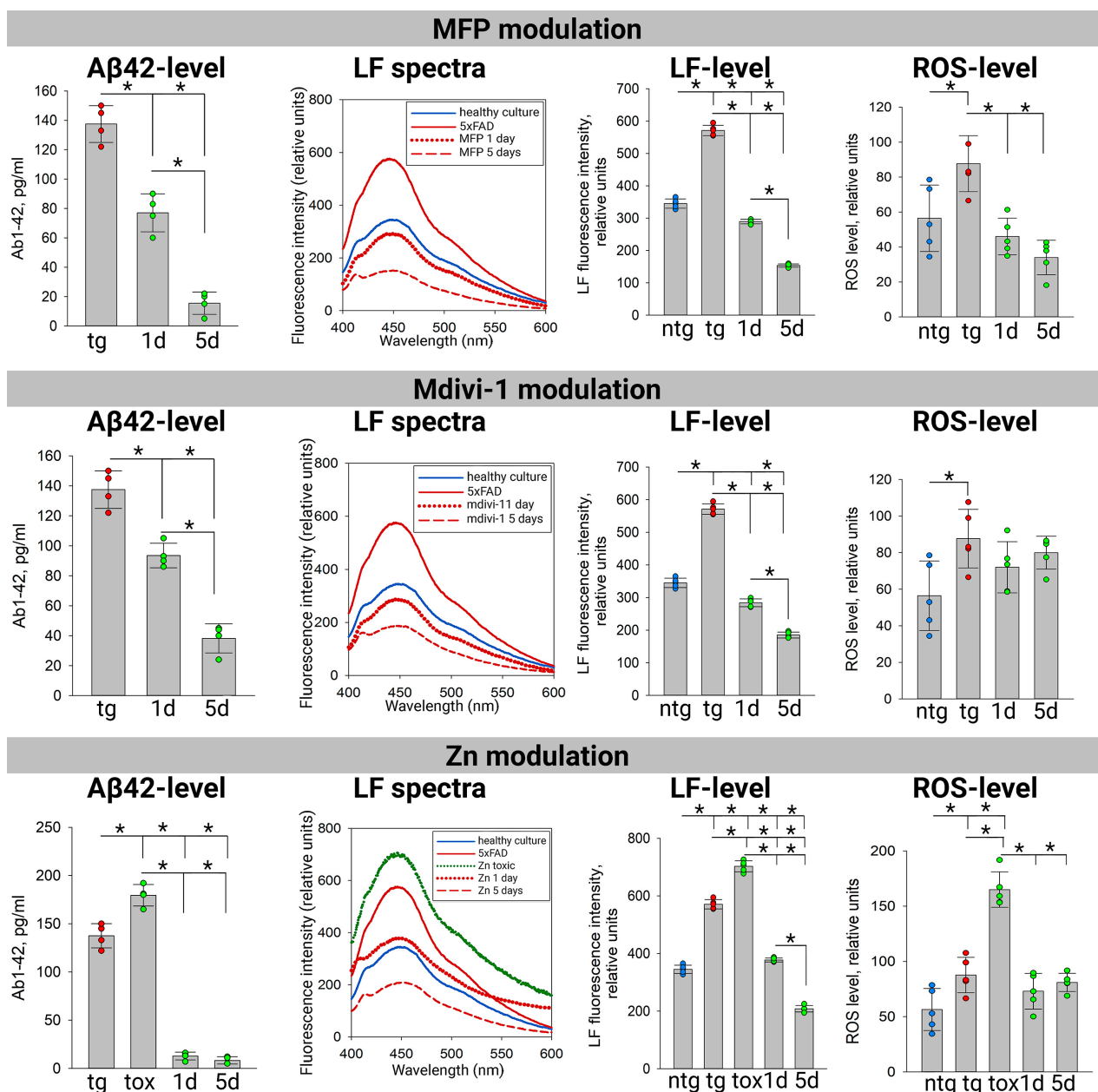


**Fig. 2. Accumulation of beta-amyloid, lipofuscin and ROS in 5xHAD transgenic cultures under the action of mitochondrial dynamics modulators.** Aβ1-42 levels in cell cultures were evaluated using ELISA. Lipofuscin accumulation and ROS levels were assessed fluorimetrically. Accumulation of lipofuscin levels also presented as fluorescence spectra (Ex. 360/Em. max 450). \*  $p \leq 0.05$ , Kruskal–Wallis test, Bonferroni method. ntg, cultures derived from nontransgenic animals; tg, cultures derived from 5xHAD transgenic animals; 1d, 1 day of exposure to the tested compound; 5d, 5 days of exposure; tox, 1 day of exposure to a toxic concentration of the compound. ROS, reactive oxygen species; LF, lipofuscin; Aβ, beta-amyloid.

dropped to levels markedly below those of untreated non-transgenic cultures. A similar trend was observed following inhibition of mitochondrial fission. Fluorescence intensity in Mdivi1—1 day treated cultures ( $284 \pm 12$  r.e.) was comparable to the control group, while by day 5 ( $185 \pm 9$  r.e.), lipofuscin accumulation was significantly reduced relative to untreated transgenic cultures. The reduction observed as early as day 1, with further decline by day 5, sug-

gests that mitochondrial fusion promotes cellular clearance mechanisms, possibly through enhanced mitophagy and autophagy activation [83]. Conversely, toxic zinc overload ( $702.7 \pm 19$  r.e.) led to a dramatic increase in lipofuscin fluorescence, exceeding levels in untreated transgenic cultures. In contrast, low-dose zinc exposure produced a biphasic effect: after one day ( $377.5 \pm 7$  r.e.), lipofuscin levels were slightly elevated compared to nontransgenic



controls but remained significantly lower than in transgenic cultures, while by day 5 ( $208.1 \pm 11$  r.e.), lipofuscin fluorescence had further decreased.

In untreated 5xFAD transgenic cultures, A $\beta$ 42 accumulation reached  $137.5 \pm 12.6$  pg/mL. Treatment with MFP M1 resulted in a progressive decline in A $\beta$ 42 levels. By day 1 ( $77 \pm 13$  pg/mL), A $\beta$ 42 was significantly reduced compared to untreated transgenic cultures, and by day 5 the effect was even more pronounced ( $15.5 \pm 7.6$  pg/mL). Inhibition of mitochondrial fission with Mdivi-1 also reduced A $\beta$ 42 accumulation. After 1 day of treatment ( $93.5 \pm 8.2$  pg/mL), A $\beta$ 42 levels were already lower than in untreated transgenic cultures, and by day 5 ( $38.3 \pm 9.7$  pg/mL), they had further declined. The observed reduction in A $\beta$  levels following MFP M1 and Mdivi-1 treatment is consistent with previous reports linking mitochondrial function to amyloid clearance. The progressive decline in A $\beta$  over five days suggests that improved mitochondrial function facilitates more efficient proteostasis, potentially through enhanced autophagy and lysosomal degradation. In contrast, toxic zinc exposure ( $179.5 \pm 11.1$  pg/mL) significantly increases A $\beta$ 42 levels, exacerbating A $\beta$  pathology in line with previous findings [84,85]. This suggests that excessive zinc disrupts mechanisms involved in amyloid clearance, potentially through mitochondrial dysfunction and lysosomal impairment. Interestingly, low-dose zinc exposure had a striking effect: after 1 day ( $12.8 \pm 4$  pg/mL) and 5 days ( $8.3 \pm 3.8$  pg/mL), A $\beta$ 42 levels were nearly undetectable by our methods, suggesting that mild zinc modulation may enhance amyloid clearance. This finding warrants further investigation into the dose-dependent effects of zinc on amyloid metabolism [86,87].

The role of zinc in AD pathogenesis remains controversial. While some studies suggest therapeutic potential for zinc chelators [88,89], others report protective effects of Zn-enriched diets [87,90]. A major mechanism of zinc neurotoxicity is its ability to accelerate A $\beta$  aggregation and promote the formation of highly toxic Zn-A $\beta$  oligomers [84,91–93]. Amyloid plaques contain abnormally high Zn concentrations, long regarded as pathogenic, although alternative views propose a protective role for such accumulation [94]. Beyond its interaction with A $\beta$ , zinc is an essential regulator of neurotransmission, neurotrophism, and synaptic plasticity [95]. Sequestration of Zn into extracellular amyloid deposits depletes intracellular pools, destabilizing microtubules, promoting neurofibrillary tangle (NFT) formation, and impairing cytoskeletal integrity [85,96]. Zn deficiency also facilitates calcium influx through NMDA receptors, exacerbating oxidative stress [97]. Conversely, zinc can promote A $\beta$  clearance by directly modulating protease activity and indirectly enhancing protease expression [98], indeed, many A $\beta$ -degrading enzymes are Zn metalloproteases [99]. In addition, Zn exerts anti-inflammatory and antioxidant effects by inducing metallothioneins [99], cysteine-rich proteins with strong cytoprotective proper-

ties [100–102]. One prevailing hypothesis is that sequestration of Zn within plaques creates a state of local functional deficiency despite elevated total Zn levels, thereby contributing to glutamatergic excitotoxicity and synaptic dysfunction [95]. Data from cell models further indicate that Zn's actions depend on concentration and localization: ionophores suppress  $\alpha$ - and  $\beta$ -secretase-dependent APP processing [103], whereas the chelator clioquinol, by increasing intracellular Zn, activates matrix metalloproteinases and reduces A $\beta$  burden. Together, these findings highlight the context-dependent nature of zinc signaling, where the same element can exert either toxic or protective effects depending on dose, compartmentalization, and baseline cellular environment.

ROS levels followed a pattern consistent with mitochondrial dysfunction in 5xFAD transgenic cultures, showing a significant increase compared to nontransgenic controls. In nontransgenic cultures ( $56.4 \pm 19$  r.e.), ROS levels remained low, whereas untreated 5xFAD transgenic cultures ( $87.7 \pm 16$  r.e.) exhibited a marked elevation, consistent with the well-documented mitochondrial dysfunction and oxidative stress associated with Alzheimer's disease pathology. Treatment with MFP M1 produced a progressive reduction in ROS. After 1 day ( $46 \pm 10.5$  r.e.), ROS levels dropped below those of transgenic cultures, suggesting an early antioxidative effect. By day 5 ( $34 \pm 9.9$  r.e.), ROS levels were further reduced, indicating that enhanced mitochondrial fusion supports redox balance, possibly by optimizing mitochondrial function and ATP production. Hyperfusion of mitochondria have been observed to transiently lower intracellular ROS levels, accompanied by reduced oxygen consumption and ATP synthesis, which typically recover to baseline after a period of time [104,105]. Inhibition of mitochondrial fission with Mdivi-1 produced more variable effects on ROS levels. After 1 day, ROS levels were ( $72 \pm 14$  r.e.), and by day 5 ( $80 \pm 9$  r.e.), they had returned to values similar to untreated transgenic cultures. We found no significant differences between both mdivi-ntg and mdivi-tg groups. Previous studies have reported that repeated daily Mdivi-1 treatment lower ROS levels [106]. However, Mdivi-1 is also known to increase ROS [75], triggering mitochondrial retrograde signaling [53], which may have broader implications beyond its role in mitochondrial dynamic. Toxic zinc overload ( $165 \pm 16$  r.e.) caused a sharp increase in ROS levels, reinforcing its role in exacerbating oxidative stress. Low-dose zinc exposure showed that after 1 day, ROS levels were  $73.0 \pm 16.2$  r.e., and by day 5, ROS levels were  $81.0 \pm 8.2$  r.e. We found no significant differences between Zn-ntg and Zn-tg groups.

### 3.3 Neuronal and Astrocytic Morphology and the Impact of Mitochondrial Dynamics on Cellular Organization

As shown in Fig. 3, transgenic 5xFAD and nontransgenic cultures exhibit distinct morphological characteris-



tics despite being prepared under identical culture conditions. 5xFAD cultures are characterized by pronounced astrogliosis ( $54.2 \pm 5\%$  in nontransgenic cultures vs.  $70 \pm 7.3\%$  in 5xFAD cultures), accompanied by a reduction in neuronal area ( $49.2 \pm 5.7\%$  in nontransgenic cultures vs.  $36.6 \pm 4.5\%$  in 5xFAD cultures) [107]. In addition, transgenic cultures tend to display a more mosaic-like organization, whereas nontransgenic cultures predominantly form clustered structures.

Treatment with the mitochondrial fission inhibitor Mdivi-1 led to a significant increase in neuronal density after one day ( $44.0 \pm 7\%$ ), which remained stable by day 5 ( $46.9 \pm 6\%$ ). A notable reduction in astrocytic area was observed by day 5, approaching levels seen in nontransgenic controls ( $70.2 \pm 6.8\%$  at day 1 vs.  $52.7 \pm 7.5\%$  at day 5). These findings suggest that Mdivi-1 promotes neuronal survival while simultaneously reducing reactive astrogliosis [108,109]. Since excessive mitochondrial fission is typically associated with cellular stress and apoptosis, the stabilization of neuronal density under Mdivi-1 treatment implies a shift toward a more balanced mitochondrial state. Interestingly, despite the increased mitochondrial fragmentation observed in treated cultures, ROS levels did not rise significantly. This apparent paradox may indicate that Mdivi-1-induced fragmentation reflects adaptive remodeling that supports mitochondrial turnover and redistribution rather than pathological degradation. The concurrent reduction in astrocytic density supports the idea that Mdivi-1 mitigates neuroinflammation by suppressing excessive glial activation.

Exposure to high concentrations of exogenous zinc, a known mitochondrial fission activator, resulted in marked neurotoxicity. Neuritic degeneration was evident (neuronal density  $25.2 \pm 4.1\%$ ), along with a moderate reduction in astrocytic density ( $60.3 \pm 6.2\%$ ). This neurotoxicity is likely due to excessive mitochondrial fragmentation, leading to energy deficits and increased oxidative stress. Astrocytic damage was particularly pronounced and consistent with clasmatodendrosis—a pathological fragmentation and retraction of astrocytic processes [110], typically associated with calcium dysregulation, calpain hyperactivation, and mitochondrial dysfunction [111]. Referring to our previous work on nontransgenic (ntg) cultures [70], we observed that high-dose zinc exposure did not induce the formation of clasmatodendrotic astrocytes. Since the primary distinction between these models lies in the accumulation of A $\beta$ , we propose that the presence of A $\beta$  may be a critical factor underlying this differential astrocytic response. Given the central role of astrocytes in neuronal support and A $\beta$  clearance, zinc-induced astrocytic damage likely contributes to neurodegeneration by disrupting these homeostatic functions.

In contrast, low-dose zinc exposure produced a markedly different effect. After one day, a modest decrease in astrocytic density was observed ( $66.7 \pm 6\%$ ), while neu-

ronal density remained stable ( $41.7 \pm 5\%$ ). By day 5, neuronal density had slightly increased ( $42.1 \pm 6.7\%$ ). Unlike the high-dose group, low-dose zinc did not cause overt toxicity. Instead, it appeared to induce mild astrocytic remodeling without negatively affecting neurons. These findings suggest that moderate levels of mitochondrial fission, triggered by subtoxic zinc concentrations, may contribute to cellular adaptation and homeostasis rather than injury [112,113]. The differential responses to zinc underscore the importance of mitochondrial balance, where excessive fragmentation is detrimental, but controlled fission may be beneficial.

Although the connection between mitochondrial dynamics and culture architecture appears intuitive, direct evidence has been limited. While theoretical models propose that mitochondrial behavior shapes culture morphology, empirical validation has been lacking. Our findings demonstrate that mitochondrial remodeling influences not only intracellular metabolism [114], but also the structural organization of neuron-astrocyte cultures. The changes in cellular arrangement following manipulation of fusion and fission suggest that mitochondrial dynamics affect intercellular interactions and coordinated behavior within the culture.

Variations and specificity in mitochondrial dynamics may be closely linked to particular cellular functions and requirements, differing across cell types [115]. For instance, studies have shown that mitochondrial dynamics regulate cell morphology in the developing cochlea [116]. Moreover, mitochondrial dysfunction has been associated with impaired brain development, depletion of the adult neural stem cell pool, and disruptions in both embryonic and adult neurogenesis [117]. In addition, mitochondrial dynamics are essential for regulating stem cell identity, self-renewal, and fate decisions [118]. Inactivation of the fusion protein OPA1, for example, has been shown to impair both tissue regeneration and stem cell pluripotency [119]. Further studies are needed to determine whether the observed metabolic changes are a direct consequence of mitochondrial remodeling or part of a broader cellular stress response aimed at maintaining homeostasis.

## 4. Conclusions

Even if one does not fully embrace the mitochondrial theory of Alzheimer's disease as the central paradigm, mitochondria undeniably remain among the most critical regulators of cellular health. Their ability to alter phenotype through fission and fusion directly affects cell morphology and structural organization in complex cell communities such as primary cultures of hippocampal cells. In our study, modulation of mitochondrial dynamics significantly influenced the accumulation of lipofuscin, a well-established marker of intracellular stress and aging, as well as A $\beta$ , a key pathogenic hallmark of AD, underscoring their potential as therapeutic targets in neurodegenerative dis-

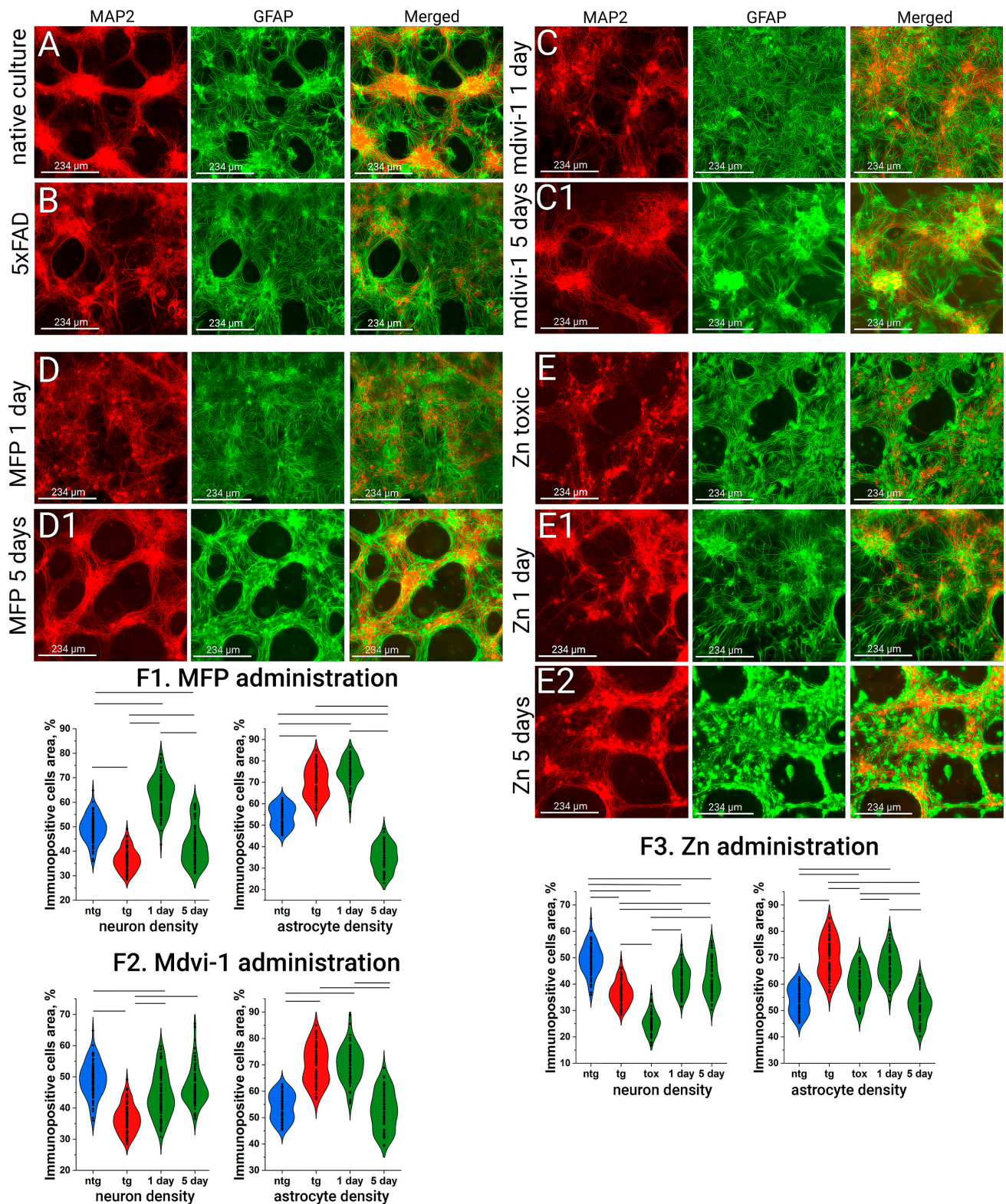


**Fig. 3. Immunopositivity to the astrocyte marker (GFAP in green) and the neuronal marker (MAP2 in red) in primary neuronal cultures under the administration of fusion and fission activators.** (A) Control non transgenic culture. (B) Control transgenic 5xFAD culture. (C,C1) Effect of Mdivi-1 on culture morphology after 1 and 5 days of administration. (D,D1) Effect of MFP M1on culture morphology after 1 and 5 days of administration. (E–E2) Effect of Zn on culture morphology after exposure to a toxic concentration and after 1 and 5 days of recovery. (F1–F3) Neuronal and astrocytic densities (in %) under the effect of MFP M1, Mdivi-1, and Zn, Lines indicate  $p \leq 0.05$ , ANOVA, Dunn test. Scale bar = 234  $\mu\text{m}$ .

eases. While controlled fusion or limited fission inhibition may support clearance pathways and cellular integrity, excessive or dysregulated fragmentation—such as that induced by zinc toxicity—can exacerbate oxidative stress and aggregate burden. Our findings provide empirical evidence that mitochondrial dynamics not only regulate intracellular metabolism but also shape structural organization and intercellular interactions within neuron-astrocyte cultures. Further research is needed to determine whether these metabolic and morphological changes arise directly from mitochondrial remodeling or as part of broader cellular stress responses aimed at preserving homeostasis.

We propose that mitochondrial morphology acts as a key regulator of both cellular homeostasis and disease pathology. Mitochondrial dynamics thus emerge as promising therapeutic targets in neurodegenerative disease models. Future research should focus on clarifying the interplay between mitochondrial remodeling and protein degradation systems (including autophagy and mitophagy), and how these interactions influence cell survival, neuroinflammation, and disease progression *in vivo*. A more comprehensive understanding of these mechanisms could facilitate the development of mitochondria-targeted strategies to restore cellular balance and delay the onset or progression of neurodegenerative disorders.

## 5. Limitation

Although Mdivi-1, MFP M1, and Zn were used to selectively modulate mitochondrial fusion and fission, these compounds may exert broader effects on cellular homeostasis. Mdivi-1, as an inhibitor of Drp1, affects not only mitochondrial fission but also peroxisomal dynamics, apoptotic signaling, and calcium homeostasis. Similarly, MFP M1, by enhancing mitochondrial fusion, may alter ER-mitochondria communication, mitophagy efficiency, and oxidative stress levels. Prolonged mitochondrial fusion could impair the clearance of dysfunctional organelles, potentially leading to secondary metabolic disturbances. Zinc, used here as a fission activator, also has well-documented effects on cellular signaling, calcium regulation, and oxidative stress. While low concentration may promote physiological fission and adaptive mitochondrial responses, excessive Zn exposure can disrupt proteostasis, enhance lipid peroxidation, and induce cytotoxicity. Future studies should therefore carefully evaluate the broader metabolic consequences of these interventions, as well as their potential off-target effects on neuronal and astrocytic functions.

Some aspects of our findings would also benefit from a complementary assessment of autophagic and mitophagic activity. The observed changes in mitochondrial morphology, ROS levels, and aggregate accumulation suggest potential alterations in mitochondrial turnover and proteostatic mechanisms; however, direct evaluation of autophagy and mitophagy markers was not included in the current study and should be addressed in future investigations.

Finally, while our *in vitro* findings provide valuable insights into the mitochondrial dynamics, their direct translation to *in vivo* conditions remains uncertain. In the brain, mitochondrial homeostasis is influenced by systemic factors, including neuroinflammation, vascular supply, and intercellular metabolic interactions, which cannot be fully replicated in primary cultures. In addition, *in vivo* pharmacokinetics may alter the efficacy and distribution of mitochondrial modulators. Future studies using whole-animal models will be necessary to assess the systemic impact of mitochondrial dynamics in Alzheimer's disease.

## Abbreviations

AD, Alzheimer's disease; ROS, reactive oxygen species; A $\beta$ , beta-amyloid; ATP, adenosine triphosphate; Mdivi-1, mitochondrial fission inhibitor-1; MFP, mitochondrial fusion promoter M1; Drp1, dynamin-related protein 1; GTP, guanosine triphosphate.

## Availability of Data and Materials

The datasets used and analyzed during the current study are available from the corresponding author on reasonable request.

## Author Contributions

AC designed the research study. AC and DZ performed the research. AC analyzed the data. AC wrote the manuscript. Both authors contributed to editorial changes in the manuscript. Both authors read and approved the final manuscript. Both authors have participated sufficiently in the work and agreed to be accountable for all aspects of the work.

## Ethics Approval and Consent to Participate

The laboratory animals were treated in accordance with the European Convention for the Protection of Vertebrates used for experimental and other purposes (Strasbourg, 1986). All animal procedures performed with mice were approved by the Bioethics Commission of the Institute of Cell Biophysics (ICB RAS, Pushchino Research Center for Biological Studies, Russian Academy of Sciences) (Approval ID: 1/032023; Date: 2023-3-22) in accordance with Directive 2010/63/EU of the European Parliament.

## Acknowledgment

The authors acknowledge institutional support from ICB RAS and IBI RAS, which provided the necessary facilities and resources for this study.

## Funding

This work was supported by the Russian Science Foundation (RSF), project No. 23-25-00485.



## Conflict of Interest

The authors declare no conflict of interest.

## Declaration of AI and AI-Assisted Technologies in the Writing Process

During the preparation of this work, the authors used ChatGPT in order to check spelling and grammar. After using this tool, the authors reviewed and edited the content as needed and take full responsibility for the content of the publication.

## Supplementary Material

Supplementary material associated with this article can be found, in the online version, at <https://doi.org/10.31083/FBL44648>.

## References

- [1] Johri A. Disentangling Mitochondria in Alzheimer's Disease. *International Journal of Molecular Sciences*. 2021; 22: 11520. <https://doi.org/10.3390/ijms222111520>.
- [2] Sharma VK, Singh TG, Mehta V. Stressed mitochondria: A target to intrude alzheimer's disease. *Mitochondrion*. 2021; 59: 48–57. <https://doi.org/10.1016/j.mito.2021.04.004>.
- [3] Tábara LC, Segawa M, Prudent J. Molecular mechanisms of mitochondrial dynamics. *Nature Reviews. Molecular Cell Biology*. 2025; 26: 123–146. <https://doi.org/10.1038/s41580-024-00785-1>.
- [4] Bell SM, Barnes K, De Marco M, Shaw PJ, Ferraiuolo L, Blackburn DJ, *et al.* Mitochondrial Dysfunction in Alzheimer's Disease: A Biomarker of the Future? *Biomedicines*. 2021; 9: 63. <https://doi.org/10.3390/biomedicines9010063>.
- [5] Adebayo M, Singh S, Singh AP, Dasgupta S. Mitochondrial fusion and fission: The fine-tune balance for cellular homeostasis. *FASEB Journal: Official Publication of the Federation of American Societies for Experimental Biology*. 2021; 35: e21620. <https://doi.org/10.1096/fj.202100067R>.
- [6] Blagov AV, Grechko AV, Nikiforov NG, Borisov EE, Sadykhov NK, Orekhov AN. Role of Impaired Mitochondrial Dynamics Processes in the Pathogenesis of Alzheimer's Disease. *International Journal of Molecular Sciences*. 2022; 23: 6954. <https://doi.org/10.3390/ijms23136954>.
- [7] Akhter F, Chen D, Yan SF, Yan SS. Mitochondrial Perturbation in Alzheimer's Disease and Diabetes. *Progress in Molecular Biology and Translational Science*. 2017; 146: 341–361. <https://doi.org/10.1016/bs.pmbts.2016.12.019>.
- [8] McCarron JG, Wilson C, Sandison ME, Olson ML, Girkin JM, Saunter C, *et al.* From structure to function: mitochondrial morphology, motion and shaping in vascular smooth muscle. *Journal of Vascular Research*. 2013; 50: 357–371. <https://doi.org/10.1159/000353883>.
- [9] Braschi E, McBride HM. Mitochondria and the culture of the Borg: understanding the integration of mitochondrial function within the reticulum, the cell, and the organism. *BioEssays: News and Reviews in Molecular, Cellular and Developmental Biology*. 2010; 32: 958–966. <https://doi.org/10.1002/bies.201000073>.
- [10] Zinina AN, Vekshin NL. Fluorometric comparison of protomitochondria and mitochondria. *Biochemistry (Moscow) Supplement Series A: Membrane and Cell Biology*. 2008; 2: 380–386. <https://doi.org/10.1134/S1990747808040120>.
- [11] Lewis TL, Jr, Kwon SK, Lee A, Shaw R, Polleux F. MFF-dependent mitochondrial fission regulates presynaptic release and axon branching by limiting axonal mitochondria size. *Nature Communications*. 2018; 9: 5008. <https://doi.org/10.1038/s41467-018-07416-2>.
- [12] Hoitzing H, Johnston IG, Jones NS. What is the function of mitochondrial networks? A theoretical assessment of hypotheses and proposal for future research. *BioEssays: News and Reviews in Molecular, Cellular and Developmental Biology*. 2015; 37: 687–700. <https://doi.org/10.1002/bies.201400188>.
- [13] Gomes LC, Di Benedetto G, Scorrano L. During autophagy mitochondria elongate, are spared from degradation and sustain cell viability. *Nature Cell Biology*. 2011; 13: 589–598. <https://doi.org/10.1038/ncb2220>.
- [14] Li A, Shami GJ, Griffiths L, Lal S, Irving H, Braet F. Giant mitochondria in cardiomyocytes: cellular architecture in health and disease. *Basic Research in Cardiology*. 2023; 118: 39. <https://doi.org/10.1007/s00395-023-01011-3>.
- [15] Hao T, Yu J, Wu Z, Jiang J, Gong L, Wang B, *et al.* Hypoxia-reprogramed megamitochondrion contacts and engulf lysosome to mediate mitochondrial self-digestion. *Nature Communications*. 2023; 14: 4105. <https://doi.org/10.1038/s41467-023-39811-9>.
- [16] Serasinghe MN, Chipuk JE. Mitochondrial Fission in Human Diseases. *Handbook of Experimental Pharmacology*. 2017; 240: 159–188. [https://doi.org/10.1007/164\\_2016\\_38](https://doi.org/10.1007/164_2016_38).
- [17] Zhu X, Perry G, Smith MA, Wang X. Abnormal mitochondrial dynamics in the pathogenesis of Alzheimer's disease. *Journal of Alzheimer's Disease: JAD*. 2013; 33 Suppl 1: S253–S262. <https://doi.org/10.3233/JAD-2012-129005>.
- [18] Wang W, Zhao F, Ma X, Perry G, Zhu X. Mitochondria dysfunction in the pathogenesis of Alzheimer's disease: recent advances. *Molecular Neurodegeneration*. 2020; 15: 30. <https://doi.org/10.1186/s13024-020-00376-6>.
- [19] Wang X, Davis RL. Early Mitochondrial Fragmentation and Dysfunction in a Drosophila Model for Alzheimer's Disease. *Molecular Neurobiology*. 2021; 58: 143–155. <https://doi.org/10.1007/s12035-020-02107-w>.
- [20] Araujo APB, Vargas G, Hayashide LDS, Matias I, Andrade CBV, de Carvalho JJ, *et al.* Aging promotes an increase in mitochondrial fragmentation in astrocytes. *Frontiers in Cellular Neuroscience*. 2024; 18: 1496163. <https://doi.org/10.3389/fncel.2024.1496163>.
- [21] Lustbader JW, Cirilli M, Lin C, Xu HW, Takuma K, Wang N, *et al.* Aβ directly links Aβeta to mitochondrial toxicity in Alzheimer's disease. *Science* 2004; 304: 448–452. <https://doi.org/10.1126/science.1091230>.
- [22] Meng X, Song Q, Liu Z, Liu X, Wang Y, Liu J. Neurotoxic β-amyloid oligomers cause mitochondrial dysfunction—the trigger for PANoptosis in neurons. *Frontiers in Aging Neuroscience*. 2024; 16: 1400544. <https://doi.org/10.3389/fnagi.2024.1400544>.
- [23] Serwer P, Wright ET, Hunter B. Additions to Alpha-Sheet Based Hypotheses for the Cause of Alzheimer's Disease. *Journal of Alzheimer's Disease: JAD*. 2022; 88: 429–438. <https://doi.org/10.3233/JAD-220311>.
- [24] Moreno-García A, Kun A, Calero O, Medina M, Calero M. An Overview of the Role of Lipofuscin in Age-Related Neurodegeneration. *Frontiers in Neuroscience*. 2018; 12: 464. <https://doi.org/10.3389/fnins.2018.00464>.
- [25] Gómez-Ramos P, Asunción Morán M. Ultrastructural localization of intraneuronal Aβeta-peptide in Alzheimer disease brains. *Journal of Alzheimer's Disease: JAD*. 2007; 11: 53–59. <https://doi.org/10.3233/jad-2007-11109>.
- [26] Chen W, Zhao H, Li Y. Mitochondrial dynamics in health and disease: mechanisms and potential targets. *Signal Transduction and Targeted Therapy*. 2023; 8: 333. <https://doi.org/10.1038/s41392-023-01547-9>.



- [27] Chen H, Lu M, Lyu Q, Shi L, Zhou C, Li M, *et al.* Mitochondrial dynamics dysfunction: Unraveling the hidden link to depression. *Biomedicine & Pharmacotherapy = Biomedicine & Pharmacotherapie*. 2024; 175: 116656. <https://doi.org/10.1016/j.biopha.2024.116656>.
- [28] Geto Z, Molla MD, Challa F, Belay Y, Getahun T. Mitochondrial Dynamic Dysfunction as a Main Triggering Factor for Inflammation Associated Chronic Non-Communicable Diseases. *Journal of Inflammation Research*. 2020; 13: 97–107. <https://doi.org/10.2147/JIR.S232009>.
- [29] Yamazaki Y, Fujii S. Extracellular ATP modulates synaptic plasticity induced by activation of metabotropic glutamate receptors in the hippocampus. *Biomedical Research (Tokyo, Japan)*. 2015; 36: 1–9. <https://doi.org/10.2220/biomedres.36.1>.
- [30] Yassine HN, Solomon V, Thakral A, Sheikh-Bahaei N, Chui HC, Braskie MN, *et al.* Brain energy failure in dementia syndromes: Opportunities and challenges for glucagon-like peptide-1 receptor agonists. *Alzheimer's & Dementia: the Journal of the Alzheimer's Association*. 2022; 18: 478–497. <https://doi.org/10.1002/alz.12474>.
- [31] Blonz ER. Alzheimer's Disease as the Product of a Progressive Energy Deficiency Syndrome in the Central Nervous System: The Neuroenergetic Hypothesis. *Journal of Alzheimer's Disease: JAD*. 2017; 60: 1223–1229. <https://doi.org/10.3233/JAD-170549>.
- [32] Chaplygina A, Zhdanova D. Mitochondrial Fragmentation as a Key Driver of Neurodegenerative Disease. *Current Alzheimer Research*. 2024; 21: 607–614. <https://doi.org/10.2174/0115672050366194250107050650>.
- [33] Liu RX, Huang C, Bennett DA, Li H, Wang R. The characteristics of astrocyte on A $\beta$  clearance altered in Alzheimer's disease were reversed by anti-inflammatory agent (+)-2-(1-hydroxyl-4-oxocyclohexyl) ethyl caffeine. *American Journal of Translational Research*. 2016; 8: 4082–4094.
- [34] Wyss-Coray T, Loike JD, Brionne TC, Lu E, Anankov R, Yan F, *et al.* Adult mouse astrocytes degrade amyloid-beta in vitro and in situ. *Nature Medicine*. 2003; 9: 453–457. <https://doi.org/10.1038/nm838>.
- [35] Nielsen HM, Veerhuis R, Holmqvist B, Janciauskiene S. Binding and uptake of A beta1-42 by primary human astrocytes in vitro. *Glia*. 2009; 57: 978–988. <https://doi.org/10.1002/glia.20822>.
- [36] D'Alessandro MCB, Kanaan S, Geller M, Praticò D, Daher JPL. Mitochondrial dysfunction in Alzheimer's disease. *Ageing Research Reviews*. 2025; 107: 102713. <https://doi.org/10.1016/j.arr.2025.102713>.
- [37] Gillardon F, Rist W, Kussmaul L, Vogel J, Berg M, Danzer K, *et al.* Proteomic and functional alterations in brain mitochondria from Tg2576 mice occur before amyloid plaque deposition. *Proteomics*. 2007; 7: 605–616. <https://doi.org/10.1002/pmic.200600728>.
- [38] de la Cueva M, Antequera D, Ordoñez-Gutierrez L, Wandosell F, Camins A, Carro E, *et al.* Amyloid- $\beta$  impairs mitochondrial dynamics and autophagy in Alzheimer's disease experimental models. *Scientific Reports*. 2022; 12: 10092. <https://doi.org/10.1038/s41598-022-13683-3>.
- [39] Bhatti JS, Kaur S, Mishra J, Dibbanti H, Singh A, Reddy AP, *et al.* Targeting dynamin-related protein-1 as a potential therapeutic approach for mitochondrial dysfunction in Alzheimer's disease. *Biochimica et Biophysica Acta. Molecular Basis of Disease*. 2023; 1869: 166798. <https://doi.org/10.1016/j.bbadis.2023.166798>.
- [40] Zacharioudakis E, Agianian B, Kumar Mv V, Biris N, Garner TP, Rabinovich-Nikitin I, *et al.* Modulating mitofusins to control mitochondrial function and signaling. *Nature Communications*. 2022; 13: 3775. <https://doi.org/10.1038/s41467-022-31324-1>.
- [41] McGill Percy KC, Liu Z, Qi X. Mitochondrial dysfunction in Alzheimer's disease: Guiding the path to targeted therapies. *Neurotherapeutics: the Journal of the American Society for Experimental NeuroTherapeutics*. 2025; 22: e00525. <https://doi.org/10.1016/j.neurot.2025.e00525>.
- [42] Chen Z, Chai E, Mou Y, Roda RH, Blackstone C, Li XJ. Inhibiting mitochondrial fission rescues degeneration in hereditary spastic paraplegia neurons. *Brain: a Journal of Neurology*. 2022; 145: 4016–4031. <https://doi.org/10.1093/brain/awab488>.
- [43] Pandey R, Bisht P, Kumari A, Ray A, Ravichandiran V, Kumar N. Targeting Mitochondrial Dynamics as a Restorative Approach in the Treatment of Alzheimer's Disease. In: Kumar D, Patil VM, Wu D, Thorat N (eds.) *Deciphering Drug Targets for Alzheimer's Disease* (pp. 181–197). Springer Nature Singapore: Singapore. 2023. [https://doi.org/10.1007/978-981-99-2657-2\\_9](https://doi.org/10.1007/978-981-99-2657-2_9).
- [44] Lanzillotta C, Di Domenico F, Perluigi M, Butterfield DA. Targeting Mitochondria in Alzheimer Disease: Rationale and Perspectives. *CNS Drugs*. 2019; 33: 957–969. <https://doi.org/10.1007/s40263-019-00658-8>.
- [45] Atlante A, Amadoro G, Latina V, Valenti D. Therapeutic Potential of Targeting Mitochondria for Alzheimer's Disease Treatment. *Journal of Clinical Medicine*. 2022; 11: 6742. <https://doi.org/10.3390/jcm11226742>.
- [46] Trushina E, Nemutlu E, Zhang S, Christensen T, Camp J, Mesa J, *et al.* Defects in mitochondrial dynamics and metabolomic signatures of evolving energetic stress in mouse models of familial Alzheimer's disease. *PloS One*. 2012; 7: e32737. <https://doi.org/10.1371/journal.pone.0032737>.
- [47] Sharma N, Banerjee R, Davis RL. Early Mitochondrial Defects in the 5xFAD Mouse Model of Alzheimer's Disease. *Journal of Alzheimer's Disease: JAD*. 2023; 91: 1323–1338. <https://doi.org/10.3233/JAD-220884>.
- [48] Reddy PH, Oliver DM. Amyloid Beta and Phosphorylated Tau-Induced Defective Autophagy and Mitophagy in Alzheimer's Disease. *Cells*. 2019; 8: 488. <https://doi.org/10.3390/cell8050488>.
- [49] Wang W, Yin J, Ma X, Zhao F, Siedlak SL, Wang Z, *et al.* Inhibition of mitochondrial fragmentation protects against Alzheimer's disease in rodent model. *Human Molecular Genetics*. 2017; 26: 4118–4131. <https://doi.org/10.1093/hmg/ddx299>.
- [50] Liu X, Song L, Yu J, Huang F, Li Y, Ma C. Mdivi-1: a promising drug and its underlying mechanisms in the treatment of neurodegenerative diseases. *Histology and Histopathology*. 2022; 37: 505–512. <https://doi.org/10.14670/HH-18-443>.
- [51] Baek SH, Park SJ, Jeong JI, Kim SH, Han J, Kyung JW, *et al.* Inhibition of Drp1 Ameliorates Synaptic Depression, A $\beta$  Deposition, and Cognitive Impairment in an Alzheimer's Disease Model. *Journal of Neuroscience*. 2017; 37: 5099–5110. <https://doi.org/10.1523/JNEUROSCI.2385-16.2017>.
- [52] Oliver D, Reddy PH. Dynamics of Dynamin-Related Protein 1 in Alzheimer's Disease and Other Neurodegenerative Diseases. *Cells*. 2019; 8: 961. <https://doi.org/10.3390/cells8090961>.
- [53] Ahn SI, Choi SK, Kim MJ, Wie J, You JS. Mdivi-1: Effective but complex mitochondrial fission inhibitor. *Biochemical and Biophysical Research Communications*. 2024; 710: 149886. <https://doi.org/10.1016/j.bbrc.2024.149886>.
- [54] Marx N, Ritter N, Disse P, Seeböhm G, Busch KB. Detailed analysis of Mdivi-1 effects on complex I and respiratory supercomplex assembly. *Scientific Reports*. 2024; 14: 19673. <https://doi.org/10.1038/s41598-024-69748-y>.
- [55] Wang D, Wang J, Bonamy GMC, Meeusen S, Brusch RG, Turk C, *et al.* A small molecule promotes mitochondrial fusion in mammalian cells. *Angewandte Chemie (International Ed. in English)*. 2012; 51: 9302–9305. <https://doi.org/10.1002/anie.201204589>.
- [56] Surinkaew P, Apaijai N, Sawaddiruk P, Jaiwongkam T,

- Kerdphoo S, Chattipakorn N, *et al.* Mitochondrial Fusion Promoter Alleviates Brain Damage in Rats with Cardiac Ischemia/Reperfusion Injury. *Journal of Alzheimer's Disease*. JAD. 2020; 77: 993–1003. <https://doi.org/10.3233/JAD-200495>.
- [57] Wang L, Liu M, Gao J, Smith AM, Fujioka H, Liang J, *et al.* Mitochondrial Fusion Suppresses Tau Pathology-Induced Neurodegeneration and Cognitive Decline. *Journal of Alzheimer's Disease*. JAD. 2021; 84: 1057–1069. <https://doi.org/10.3233/JAD-215175>.
- [58] Sensi SL, Ton-That D, Sullivan PG, Jonas EA, Gee KR, Kaczmarek LK, *et al.* Modulation of mitochondrial function by endogenous Zn<sup>2+</sup> pools. *Proceedings of the National Academy of Sciences of the United States of America*. 2003; 100: 6157–6162. <https://doi.org/10.1073/pnas.1031598100>.
- [59] Qi Z, Shi W, Zhao Y, Ji X, Liu KJ. Zinc accumulation in mitochondria promotes ischemia-induced BBB disruption through Drp1-dependent mitochondria fission. *Toxicology and Applied Pharmacology*. 2019; 377: 114601. <https://doi.org/10.1016/j.taap.2019.114601>.
- [60] Bowers K, Srai SKS. The trafficking of metal ion transporters of the Zrt- and Irt-like protein family. *Traffic (Copenhagen, Denmark)*. 2018; 19: 813–822. <https://doi.org/10.1111/tra.12602>.
- [61] Chipuk JE. Think We Understand the Role of DRP1 in Mitochondrial Biology? Zinc Again!. *Molecular Cell*. 2019; 73: 197–198. <https://doi.org/10.1016/j.molcel.2018.12.024>.
- [62] Yang Q, Yang J, Liu X, Zhang Y, Li Y, Ao D, *et al.* Crosstalk Between the Mitochondrial Dynamics and Oxidative Stress in Zinc-induced Cytotoxicity. *Biological Trace Element Research*. 2023; 201: 4419–4428. <https://doi.org/10.1007/s12011-022-03504-z>.
- [63] Knies KA, Li YV. Zinc cytotoxicity induces mitochondrial morphology changes in hela cell line. *International Journal of Physiology, Pathophysiology and Pharmacology*. 2021; 13: 43–51.
- [64] Sprenger HG, Langer T. The Good and the Bad of Mitochondrial Breakups. *Trends in Cell Biology*. 2019; 29: 888–900. <https://doi.org/10.1016/j.tcb.2019.08.003>.
- [65] Suen DF, Norris KL, Youle RJ. Mitochondrial dynamics and apoptosis. *Genes & Development*. 2008; 22: 1577–1590. <https://doi.org/10.1101/gad.1658508>.
- [66] Tondera D, Grandemange S, Jourdain A, Karbowski M, Mattenberger Y, Herzig S, *et al.* SLP-2 is required for stress-induced mitochondrial hyperfusion. *The EMBO Journal*. 2009; 28: 1589–1600. <https://doi.org/10.1038/emboj.2009.89>.
- [67] Twig G, Hyde B, Shirihai OS. Mitochondrial fusion, fission and autophagy as a quality control axis: the bioenergetic view. *Biochimica et Biophysica Acta*. 2008; 1777: 1092–1097. <https://doi.org/10.1016/j.bbabi.2008.05.001>.
- [68] Lyamzaev KG, Izumov DS, Avetisyan AV, Yang F, Pletjushkina OY, Chernyak BV. Inhibition of mitochondrial bioenergetics: the effects on structure of mitochondria in the cell and on apoptosis. *Acta Biochimica Polonica*. 2004; 51: 553–562.
- [69] Pletjushkina OY, Lyamzaev KG, Popova EN, Nepryakhina OK, Ivanova OY, Domnina LV, *et al.* Effect of oxidative stress on dynamics of mitochondrial reticulum. *Biochimica et Biophysica Acta*. 2006; 1757: 518–524. <https://doi.org/10.1016/j.bbabi.2006.03.018>.
- [70] Chaplygina AV, Zhdanova DY. Effects of mitochondrial fusion and fission regulation on mouse hippocampal primary cultures: relevance to Alzheimer's disease. *Aging Pathobiology and Therapeutics*. 2024; 6: 8–17. <https://doi.org/10.31491/APT.2024.03.132>.
- [71] Kikugawa K, Kato T, Beppu M, Hayasaka A. Fluorescent and cross-linked proteins formed by free radical and aldehyde species generated during lipid oxidation. *Advances in Experimental Medicine and Biology*. 1989; 266: 345–56; discussion 357. [https://doi.org/10.1007/978-1-4899-5339-1\\_25](https://doi.org/10.1007/978-1-4899-5339-1_25).
- [72] Chaplygina AV, Kovalev VI, Zhdanova DY. The study of lipofuscin levels in the 5xFAD mouse model of Alzheimer's disease. *Advances in Gerontology = Uspekhi Gerontologii*. 2023; 36: 720–728. (In Russian)
- [73] Vekshin NL. Spectrophotometric determination of the quantity of protein in standard biological suspensions. *Nauchnye Doklady Vysshei Shkoly. Biologicheskie Nauki*. 1988; 107–111.
- [74] Shang Y, Li Z, Cai P, Li W, Xu Y, Zhao Y, *et al.* Megamitochondria plasticity: Function transition from adaption to disease. *Mitochondrion*. 2023; 71: 64–75. <https://doi.org/10.1016/j.mito.2023.06.001>.
- [75] Bordt EA, Clerc P, Roelofs BA, Saladino AJ, Tretter L, Adam-Vizi V, *et al.* The Putative Drp1 Inhibitor mdivi-1 Is a Reversible Mitochondrial Complex I Inhibitor that Modulates Reactive Oxygen Species. *Developmental Cell*. 2017; 40: 583–594.e6. <https://doi.org/10.1016/j.devcel.2017.02.020>.
- [76] Jiang X, Jiang H, Shen Z, Wang X. Activation of mitochondrial protease OMA1 by Bax and Bak promotes cytochrome c release during apoptosis. *Proceedings of the National Academy of Sciences of the United States of America*. 2014; 111: 14782–14787. <https://doi.org/10.1073/pnas.1417253111>.
- [77] Roy M, Itoh K, Iijima M, Sesaki H. Parkin suppresses Drp1-independent mitochondrial division. *Biochemical and Biophysical Research Communications*. 2016; 475: 283–288. <https://doi.org/10.1016/j.bbrc.2016.05.038>.
- [78] Fenton AR, Jongens TA, Holzbaur ELF. Mitochondrial dynamics: Shaping and remodeling an organelle network. *Current Opinion in Cell Biology*. 2021; 68: 28–36. <https://doi.org/10.1016/j.ceb.2020.08.014>.
- [79] Yamashita SI, Jin X, Furukawa K, Hamasaki M, Nezu A, Otera H, *et al.* Mitochondrial division occurs concurrently with autophagosome formation but independently of Drp1 during mitophagy. *The Journal of Cell Biology*. 2016; 215: 649–665. <https://doi.org/10.1083/jcb.201605093>.
- [80] Pon LA. Mitochondrial fission: rings around the organelle. *Current Biology: CB*. 2013; 23: R279–R281. <https://doi.org/10.1016/j.cub.2013.02.042>.
- [81] Steffen J, Koehler CM. ER-mitochondria contacts: Actin dynamics at the ER control mitochondrial fission via calcium release. *The Journal of Cell Biology*. 2018; 217: 15–17. <https://doi.org/10.1083/jcb.201711075>.
- [82] Aishwarya R, Alam S, Abdullah CS, Morshed M, Nitu SS, Pan-chatcharam M, *et al.* Pleiotropic effects of mdivi-1 in altering mitochondrial dynamics, respiration, and autophagy in cardiomyocytes. *Redox Biology*. 2020; 36: 101660. <https://doi.org/10.1016/j.redox.2020.101660>.
- [83] Song SB, Shim W, Hwang ES. Lipofuscin Granule Accumulation Requires Autophagy Activation. *Molecules and Cells*. 2023; 46: 486–495. <https://doi.org/10.14348/molcells.2023.0019>.
- [84] Lee MC, Yu WC, Shih YH, Chen CY, Guo ZH, Huang SJ, *et al.* Zinc ion rapidly induces toxic, off-pathway amyloid- $\beta$  oligomers distinct from amyloid- $\beta$  derived diffusible ligands in Alzheimer's disease. *Scientific Reports*. 2018; 8: 4772. <https://doi.org/10.1038/s41598-018-23122-x>.
- [85] Grabrucker AM, Schmeisser MJ, Udvardi PT, Arons M, Schoen M, Woodling NS, *et al.* Amyloid beta protein-induced zinc sequestration leads to synaptic loss via dysregulation of the ProSAP2/Shank3 scaffold. *Molecular Neurodegeneration*. 2011; 6: 65. <https://doi.org/10.1186/1750-1326-6-65>.
- [86] Corona C, Masciopinto F, Silvestri E, Viscovo AD, Lattanzio R, Sorda RL, *et al.* Dietary zinc supplementation of 3xTg-AD mice increases BDNF levels and prevents cognitive deficits as well as mitochondrial dysfunction. *Cell Death & Disease*. 2010; 1: e91. <https://doi.org/10.1038/cddis.2010.73>.
- [87] Squitti R, Pal A, Picozza M, Avan A, Ventriglia M, Rongioletti

- MC, *et al.* Zinc Therapy in Early Alzheimer's Disease: Safety and Potential Therapeutic Efficacy. *Biomolecules*. 2020; 10: 1164. <https://doi.org/10.3390/biom10081164>.
- [88] Cherny RA, Atwood CS, Xilinas ME, Gray DN, Jones WD, McLean CA, *et al.* Treatment with a copper-zinc chelator markedly and rapidly inhibits beta-amyloid accumulation in Alzheimer's disease transgenic mice. *Neuron*. 2001; 30: 665–676. [https://doi.org/10.1016/s0896-6273\(01\)00317-8](https://doi.org/10.1016/s0896-6273(01)00317-8).
- [89] Fasae KD, Abolaji AO, Faloye TR, Odunsi AY, Oyeyayo BO, Enya JI, *et al.* Metallobiology and therapeutic chelation of biomaterials (copper, zinc and iron) in Alzheimer's disease: Limitations, and current and future perspectives. *Journal of Trace Elements in Medicine and Biology: Organ of the Society for Minerals and Trace Elements (GMS)*. 2021; 67: 126779. <https://doi.org/10.1016/j.jtemb.2021.126779>.
- [90] Rivers-Auty J, Tapia VS, White CS, Daniels MJ, Drinkall S, Kennedy PT, *et al.* Zinc Status Alters Alzheimer's Disease Progression through NLRP3-Dependent Inflammation. *Journal of Neuroscience*. 2021; 41: 3025–3038. <https://doi.org/10.1523/JNEUROSCI.1980-20.2020>.
- [91] Rana M, Sharma AK. Cu and Zn interactions with A $\beta$  peptides: consequence of coordination on aggregation and formation of neurotoxic soluble A $\beta$  oligomers. *Metallomics: Integrated Biomaterial Science*. 2019; 11: 64–84. <https://doi.org/10.1039/c8mt00203g>.
- [92] Ataman Sadik D, Cansız CS, Turğut M, Dağ Ç, Duman M. Investigation of Methylsulfonamide's Capability to Prevent Zn<sup>2+</sup>-Induced A $\beta$  Peptide Aggregation Based on Zn<sup>2+</sup> Coordination within the Zinc Binding Region of A $\beta$  for Treatment of Alzheimer's Disease (AD). *ACS Chemical Neuroscience*. 2025; 16: 2945–2957. <https://doi.org/10.1021/acschemneuro.5c00238>.
- [93] Dong J, Shokes JE, Scott RA, Lynn DG. Modulating amyloid self-assembly and fibril morphology with Zn(II). *Journal of the American Chemical Society*. 2006; 128: 3540–3542. <https://doi.org/10.1021/ja055973j>.
- [94] Cuajungco MP, Goldstein LE, Nunomura A, Smith MA, Lim JT, Atwood CS, *et al.* Evidence that the beta-amyloid plaques of Alzheimer's disease represent the redox-silencing and entombment of A $\beta$  by zinc. *The Journal of Biological Chemistry*. 2000; 275: 19439–19442. <https://doi.org/10.1074/jbc.C000165200>.
- [95] Sensi SL, Granzotto A, Siotto M, Squitti R. Copper and Zinc Dysregulation in Alzheimer's Disease. *Trends in Pharmacological Sciences*. 2018; 39: 1049–1063. <https://doi.org/10.1016/j.tips.2018.10.001>.
- [96] Craddock TJA, Tuszyński JA, Chopra D, Casey N, Goldstein LE, Hameroff SR, *et al.* The zinc dyshomeostasis hypothesis of Alzheimer's disease. *PLoS One*. 2012; 7: e33552. <https://doi.org/10.1371/journal.pone.0033552>.
- [97] Aimo L, Cherr GN, Oteiza PI. Low extracellular zinc increases neuronal oxidant production through nadph oxidase and nitric oxide synthase activation. *Free Radical Biology & Medicine*. 2010; 48: 1577–1587. <https://doi.org/10.1016/j.freeradbiomed.2010.02.040>.
- [98] Grasso G, Giuffrida ML, Rizzarelli E. Metallostasis and amyloid  $\beta$ -degrading enzymes. *Metallomics: Integrated Biomaterial Science*. 2012; 4: 937–949. <https://doi.org/10.1039/c2mt0105d>.
- [99] Watt NT, Whitehouse IJ, Hooper NM. The role of zinc in Alzheimer's disease. *International Journal of Alzheimer's Disease*. 2010; 2011: 971021. <https://doi.org/10.4061/2011/971021>.
- [100] Temnik M, Rudyk M, Balakin A, Gurin S, Dovbychnuk T, Byshovets R, *et al.* Anti-inflammatory effects of <sup>64</sup>Zn-aspartate is accompanied by cognitive improvements in rats with A $\beta$ <sub>1–40</sub>-induced alzheimer disease. *Scientific Reports*. 2025; 15: 14272. <https://doi.org/10.1038/s41598-025-97830-6>.
- [101] Fujie T, Segawa Y, Uehara A, Nakamura T, Kimura T, Yoshida E, *et al.* Zinc diethyldithiocarbamate as an inducer of metallothionein in cultured vascular endothelial cells. *The Journal of Toxicological Sciences*. 2016; 41: 217–224. <https://doi.org/10.2131/jts.41.217>.
- [102] Jarosz M, Olbert M, Wyszogrodzka G, Młyniec K, Librowski T. Antioxidant and anti-inflammatory effects of zinc. Zinc-dependent NF- $\kappa$ B signaling. *Inflammopharmacology*. 2017; 25: 11–24. <https://doi.org/10.1007/s10787-017-0309-4>.
- [103] Lee J, Kim CH, Kim DG, Ahn YS. Zinc Inhibits Amyloid beta Production from Alzheimer's Amyloid Precursor Protein in SH-SY5Y Cells. *The Korean Journal of Physiology & Pharmacology: Official Journal of the Korean Physiological Society and the Korean Society of Pharmacology*. 2009; 13: 195–200. <https://doi.org/10.4196/kjpp.2009.13.3.195>.
- [104] Wakabayashi T. Megamitochondria formation - physiology and pathology. *Journal of Cellular and Molecular Medicine*. 2002; 6: 497–538. <https://doi.org/10.1111/j.1582-4934.2002.tb00452.x>.
- [105] Wakabayashi T. Structural changes of mitochondria related to apoptosis: swelling and megamitochondria formation. *Acta Biochimica Polonica*. 1999; 46: 223–237.
- [106] Xie N, Wang C, Wu C, Cheng X, Gao Y, Zhang H, *et al.* Mdivi-1 Protects Epileptic Hippocampal Neurons from Apoptosis via Inhibiting Oxidative Stress and Endoplasmic Reticulum Stress in Vitro. *Neurochemical Research*. 2016; 41: 1335–1342. <https://doi.org/10.1007/s11064-016-1835-y>.
- [107] van Gijssel-Bonnello M, Baranger K, Benech P, Rivera S, Khrestchatsky M, de Reggi M, *et al.* Metabolic changes and inflammation in cultured astrocytes from the 5xFAD mouse model of Alzheimer's disease: Alleviation by pantethine. *PLoS One*. 2017; 12: e0175369. <https://doi.org/10.1371/journal.pone.0175369>.
- [108] Li G, Cao Y, Shen F, Wang Y, Bai L, Guo W, *et al.* Mdivi-1 Inhibits Astrocyte Activation and Astroglial Scar Formation and Enhances Axonal Regeneration after Spinal Cord Injury in Rats. *Frontiers in Cellular Neuroscience*. 2016; 10: 241. <https://doi.org/10.3389/fncel.2016.00241>.
- [109] Chung CL, Huang YH, Lin CJ, Chong YB, Wu SC, Chai CY, *et al.* Therapeutic Effect of Mitochondrial Division Inhibitor-1 (Mdivi-1) on Hyperglycemia-Exacerbated Early and Delayed Brain Injuries after Experimental Subarachnoid Hemorrhage. *International Journal of Molecular Sciences*. 2022; 23: 6924. <https://doi.org/10.3390/ijms23136924>.
- [110] Balaban D, Miyawaki EK, Bhattacharyya S, Torre M. The phenomenon of clasmotodendrosis. *Heliyon*. 2021; 7: e07605. <https://doi.org/10.1016/j.heliyon.2021.e07605>.
- [111] Guo D, Du Y, Wu Q, Jiang W, Bi H. Disrupted calcium homeostasis is involved in elevated zinc ion-induced photoreceptor cell death. *Archives of Biochemistry and Biophysics*. 2014; 560: 44–51. <https://doi.org/10.1016/j.abb.2014.07.014>.
- [112] Zhang G, Sheng M, Wang J, Teng T, Sun Y, Yang Q, *et al.* Zinc improves mitochondrial respiratory function and prevents mitochondrial ROS generation at reperfusion by phosphorylating STAT3 at Ser<sup>727</sup>. *Journal of Molecular and Cellular Cardiology*. 2018; 118: 169–182. <https://doi.org/10.1016/j.yjmcc.2018.03.019>.
- [113] Bai M, Cui Y, Sang Z, Gao S, Zhao H, Mei X. Zinc ions regulate mitochondrial quality control in neurons under oxidative stress and reduce PANoptosis in spinal cord injury models via the Lgals3-Bax pathway. *Free Radical Biology & Medicine*. 2024; 221: 169–180. <https://doi.org/10.1016/j.freeradbiomed.2024.05.037>.
- [114] Campello S, Scorrano L. Mitochondrial shape changes: orchestrating cell pathophysiology. *EMBO Reports*. 2010; 11: 678–684. <https://doi.org/10.1038/embor.2010.115>.
- [115] Kuznetsov AV, Hermann M, Saks V, Hengster P, Margreiter

- R. The cell-type specificity of mitochondrial dynamics. *The International Journal of Biochemistry & Cell Biology*. 2009; 41: 1928–1939. <https://doi.org/10.1016/j.biocel.2009.03.007>.
- [116] O’Sullivan JDB, Terry S, Scott CA, Bullen A, Jagger DJ, Mann ZF. Mitochondrial dynamics regulate cell morphology in the developing cochlea. *Development (Cambridge, England)*. 2024; 151: dev202845. <https://doi.org/10.1242/dev.202845>.
- [117] Khacho M, Clark A, Svoboda DS, MacLaurin JG, Lagace DC, Park DS, *et al.* Mitochondrial dysfunction underlies cognitive defects as a result of neural stem cell depletion and impaired neurogenesis. *Human Molecular Genetics*. 2017; 26: 3327–3341. <https://doi.org/10.1093/hmg/ddx217>.
- [118] Khacho M, Clark A, Svoboda DS, Azzi J, MacLaurin JG, Meghaizel C, *et al.* Mitochondrial Dynamics Impacts Stem Cell Identity and Fate Decisions by Regulating a Nuclear Transcriptional Program. *Cell Stem Cell*. 2016; 19: 232–247. <https://doi.org/10.1016/j.stem.2016.04.015>.
- [119] Pan X, Zhao Y, Li Y, Chen J, Zhang W, Yang L, *et al.* Mitochondrial dynamics govern whole-body regeneration through stem cell pluripotency and mitonuclear balance. *Nature Communications*. 2024; 15: 10681. <https://doi.org/10.1038/s41467-024-54720-1>.